LAND COVER REVISION THROUGH OBJECT BASED SUPERVISED CLASSIFICATION OF ASTER DATA

Alexandre Gomes, MSc student
Faculdade de Ciências, Universidade do Porto
DMA, Rua do Campo Alegre, 687
4169-007 Porto, Portugal
jalexgomes@clix.pt
André R. S. Marçal, Assistant Professor
Faculdade de Ciências, Universidade do Porto
DMA, Rua do Campo Alegre, 687
4169-007 Porto, Portugal
andre.marcal@fc.up.pt

ABSTRACT

The revision of the 1995 land cover dataset for the Vale do Sousa region, in the northwest of Portugal, was carried out by supervised classification of a multi-spectral image from the ASTER sensor. Two ASTER image granules were ortho-rectified and combined into a single multi-spectral image file, with 9 bands and a pixel resolution of 15 meters. The 9 bands used cover the spectral range from the visible to the short-wave infrared (0.52-2.43 μm). The image was initially segmented into objects at 5 hierarchical levels, of increasing size. The average object size for level 1 was 135 pixels (about 30000 m^2 or 3 ha). Training areas for 9 land cover classes (6 main classes, with 'Forest' divided into 4 sub-classes) were identified on the image segmented at this level. The previously available land cover dataset was used as a first guidance for the identification of training areas. Field surveys were carried out on these locations, with a total of 582 objects identified for training. The segmented image was classified using an algorithm based on fuzzy logic. A Maximum Likelihood classifier was also applied to the ASTER image, but on a pixel-by-pixel basis. The overall accuracy was 71.5%. The object based classification results were evaluated for forest areas, using ground verification on a total of 147 sites. An average accuracy of 46.3% was obtained. The difficulty in discriminating between the 4 'Forest' land cover classes was explored by separability analysis and unsupervised classification with hierarchical clustering.

INTRODUCTION

The production of land cover / land use maps is a common application of multi-spectral satellite images. There are numerous examples of land cover maps derived from multi-spectral satellite images such as Landsat TM and SPOT HRV. The purpose of the work presented here is to evaluate the effectiveness of ASTER (Advanced Spaceborne Thermal Emission and Reflection Radiometer) satellite data for revising the land cover dataset and to obtain updated land cover maps for the Vale do Sousa region. The most used approach is to classify each image pixel as an independent observation, regardless of its spatial context. Here we present an application where the update of the existing land cover maps was done by supervised image classification, but performed on objects grouping several image pixels.

The study area

Vale do Sousa (river Sousa valley) is a region in the Northwest of Portugal, with an area of 764 km^2 (about 300 square miles) and ground altitudes ranging from 100 to 800 meters above sea level. It is crossed by the Douro River in the south. About 70% of the region is forested or uncultivated. The uncultivated areas are mainly due to the numerous forest fires. The main forest types are eucalyptus and areas with mixed eucalyptus and pine. There are also agricultural and many small urban areas. The land structure is generally small private fields (5 ha or less) with the forest areas in

much larger portions of the land. The existing land cover dataset was produced by photo-interpretation in 1995. Only areas above 0.5 ha were classified in this dataset. This dataset was out-of-date and not very reliable. The production of updated land cover data is beneficial for the 'Forest' planning, allowing for example for the detection of burned areas and the subsequent spread of illegal species like eucalyptus.

SATELLITE DATA PRE-PROCESSING

The ASTER sensor provides multi-spectral images of the Earth with each image granule covering roughly 60 by 60 km on the ground. The ASTER images have 14 spectral bands, 3 in the visible and near infrared (VNIR instrument, 0.52-0.86 μm), 6 in the short-wave infrared (SWIR instrument, 1.60-2.43 μm) and 5 in the thermal infrared (TIR instrument, 8.12-11.65 μm) (Yamaguchi et al, 1998). The spatial resolution is 15 meters (VNIR), 30 meters (SWIR) and 90 meters (TIR). An image Data Acquisition Request (DAR) was placed at the ASTER ERSDAC WWW interface (ERSDAC, 2000). This DAR resulted in a number of image granules with partial coverage of the interest area. Two of these granules were selected, one covering the north (Path 205, Row 90, ID 408566) and one covering the south (Path 205, Row 91, ID 408567). The two granules were acquired consecutively, at 11:42, 24 October 2001. The view angle of these images was 7 degrees. The two ASTER images are both nearly 100% cloud free and combined provide complete coverage of the whole Vale do Sousa region. Only the VNIR and SWIR image bands were used, as the TIR data has a much lower spatial resolution and should not provide useful information about vegetation cover.

Geo-referencing

The ASTER images used (Level 1B) have a grid of reference points with latitude and longitude on the header files. It has been verified that an image rectification based on this points alone is reasonably accurate for flat areas, apart from a small offset that can be easily corrected. However, in mountainous regions, such as the Vale do Sousa, it is necessary to incorporate the terrain elevation in the image correction.

Ortho-rectification. The ortho-rectification of satellite images is a similar process to that applied to aerial photographs to produce ortho-photos. The OrthoEngine Satellite Edition software from PCI-Geomatics was used (PCI Geomatics, 2000). Ground Control Points were identified on each ASTER image using 1:25000 raster maps. A total of 11 Ground Control Points were identified on the image 'north' and 10 on the image 'south'. The mean RMS errors for a 2nd order model were 0.54/0.53 ('north') and 0.37/0.29 ('south') pixels. A Digital Elevation Model (DEM) of the area with a 25-meter grid was used. Each image was ortho-rectified into a 15-meter pixel geo-reference image file. Vector data with the regions road network was also available. This dataset was extracted from the 1:25000 raster maps. The accuracy of the ortho-rectified images was tested by overlaying the road vector data. Figure 1 shows a RGB composition (bands 3, 2, 1) of a section of the ortho-rectified image 'north', with the road vector data overlaid in yellow. A motorway crosses this image section, from bottom left to upper right, and a number of smaller roads are also visible. A closer inspection suggests that only minor errors are present in this section – with differences below or about the pixel size. Similar results were obtained on other sections tested for this image, and also for the ortho-rectified image 'south'.

Figure 1. Ortho-rectification verification

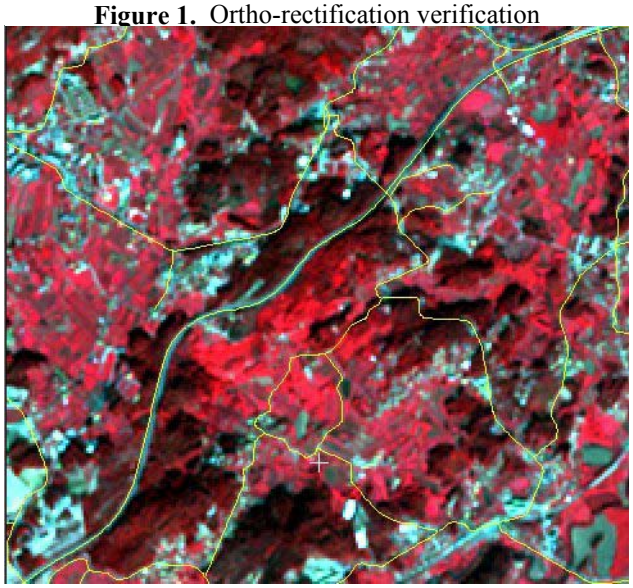

Mosaic. The two ortho-rectified images were combined into a single multi-channel image file of 2060 by 3340 15-meter pixels, that is to say 30.9 by 50.1 km, covering the whole of the Vale do Sousa region. The data from the 9 bands used, from the VNIR and SWIR instruments, were all stored in this file with a 15x15 meter pixel. The ´mosaic´ ASTER image is totally cloud free,

although there are some non-observed areas outside the Vale do Sousa region. About 75% of the interest area was provided by the 'north' image, with a much smaller contribution from the 'south' image.

Image segmentation

The ASTER image (´mosaic´) was segmented into objects using eCognition software (Baatz et al, 2001). This software allows for a multi-spectral image to be segmented, which is divided into separated regions (objects). The segmented image is produced according to the spectral signal of the pixels and their context, characterized by the objects size and shape. The homogeneity criterion is established by weighting factors for the various parameters. The values used were: color 0.8 / shape 0.2. The characterization of the shape parameter was further sub-divided into: smoothness 0.9 / compactness 0.1. The ASTER bands 1, 2 and 3 were given a weighting factor of 1 and the remaining bands were given a weighting factor of 0.1. These values were chosen to account for the different spatial resolution of the VNIR and SWIR images. The scale parameters were left with the default values for the 5 segmentation levels. Different parameter choices tend to produce slightly different results. The strategy for the identification of the "best" parameters for a particular task is not very clear. A visual inspection of a number of segmented images with different parameters, and the prior knowledge of the area was the method used to tune the segmentation parameters. The eCognition software produces a segmented image with 5 different levels structured hierarchically. Figure 2 shows an example of the various segmentation levels for a small section of the image, around the Douro River. The figure shows the segmentation levels 1 (top), 3 (middle) and 5 (bottom) overlaid on the ASTER image (RGB color composite of bands 32/12/1). The whole image was segmented into a total of 51186 objects in level 1, with an average size of 135 pixels, that is about 30000 m^2 or 3 ha. The level 2 segmentation produced 14133 objects, with an average size of 487 pixels (11 ha). The segmentation levels 3, 4 and 5 produced 4857, 2269 and 651 objects, with an average object size of 1417 pixels (32 ha), 3032 pixels (68 ha), 10569 pixels (238 ha). Taking into account the size

Figure 2. Segmented image at levels 1 (top), 3 (middle) and 5 (bottom)

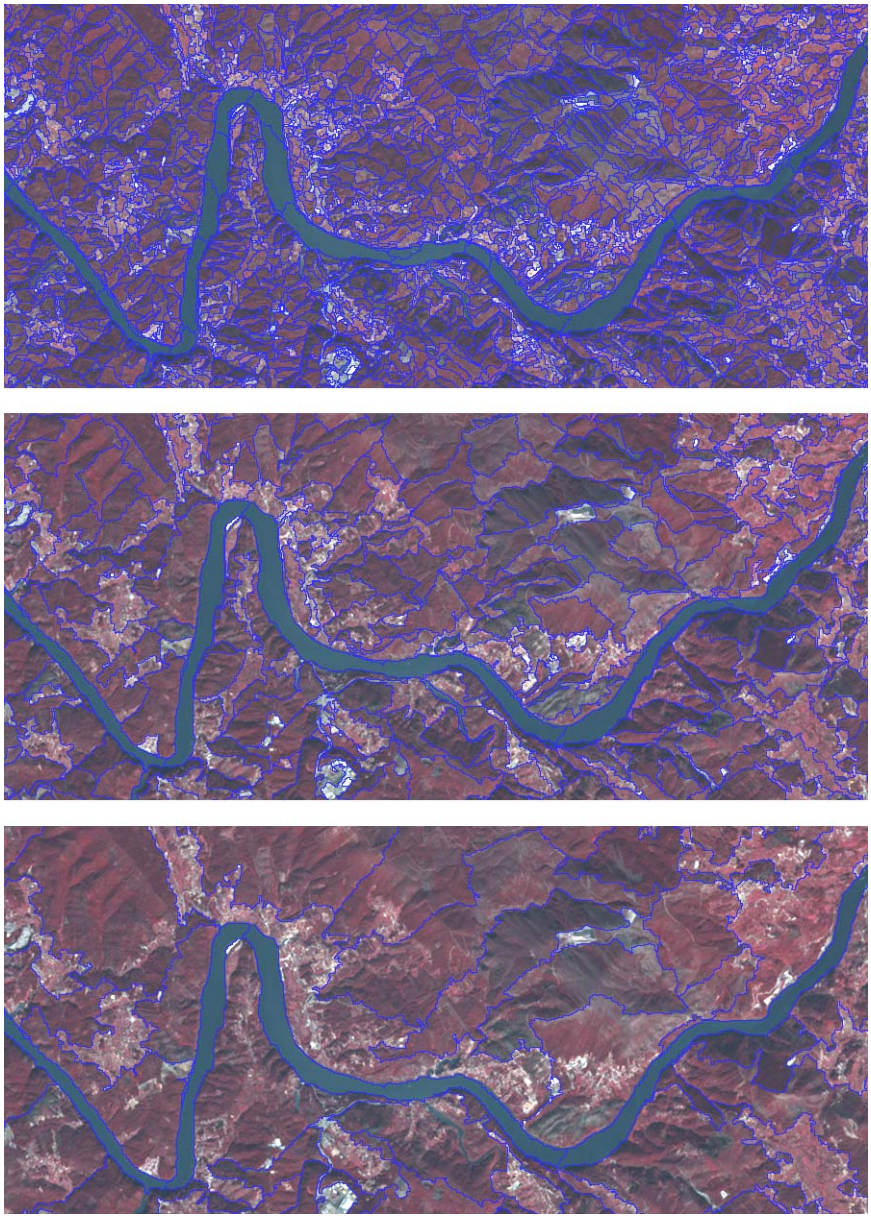

of the forest areas and small parceling of land in this part of the country, the segmentation levels 2 and 3 should be the most appropriate.

IMAGE CLASSIFICATION

The land cover classes were chosen according to the Portuguese national inventory (Tomé et al, 2002). A total of 6 main classes are used by IFN: AG – Agriculture, FL – Forest, IC – Uncultivated, IP – Non-productive, SC – Urban/Residential, HH – Water. The class Agriculture is divided in 5 sub-classes and the class Forest divided in 13 sub-classes. A different set of land cover classes was selected to suit this particular region of the country and the purpose of the study. A new class was added: 'Burned areas' (FOGO). The class 'Forest' was divided into only 4 sub-classes and the class IC used here also includes non-productive areas. A short description of the nine classes used is presented on Table 1, together with the class ID, color code and short label for each class. A simplified version was also used with only 6 main land cover classes (aggregating classes 4, 5, 6 and 7 into a single class). A void class was also used, but only to account for non-observed pixels.

Table 1. Land Cover Classes and size of training areas

Class ID	Label	Class description	No. objects	Av. size (ha)
1	SC	Urban / Residential areas	222	1.9
2	HH	Water	13	15.5
3	FOGO	Burned areas	65	3.4
4	FlEc	Forest - Eucalyptus	35	6.4
5	Flmix	Forest - mixed	70	5.8
6	FlFd	Forest - Hardwoods	12	2.6
7	FlPb	Forest - Pinus	16	4.3
8	IC	Uncultivated / Non-productive	58	5.6
9	AG	Agricultural areas	91	3.6

Training areas

Training areas were established on the segmented image at level 1. The existing land cover vector dataset, produced by photo interpretation of a 1995 air survey, was used. The polygons from this dataset that matched the segmented image polygons by at least 75% were selected as candidates for training. Ground surveys were then made to confirm the land cover of some of these objects. For practical reasons the training areas were chosen in two sectors of the image. Figure 3 shows part of the south sector, around the Douro River. The training areas are marked with the class colors, according to the color key from Table 1. A total of 582 objects were

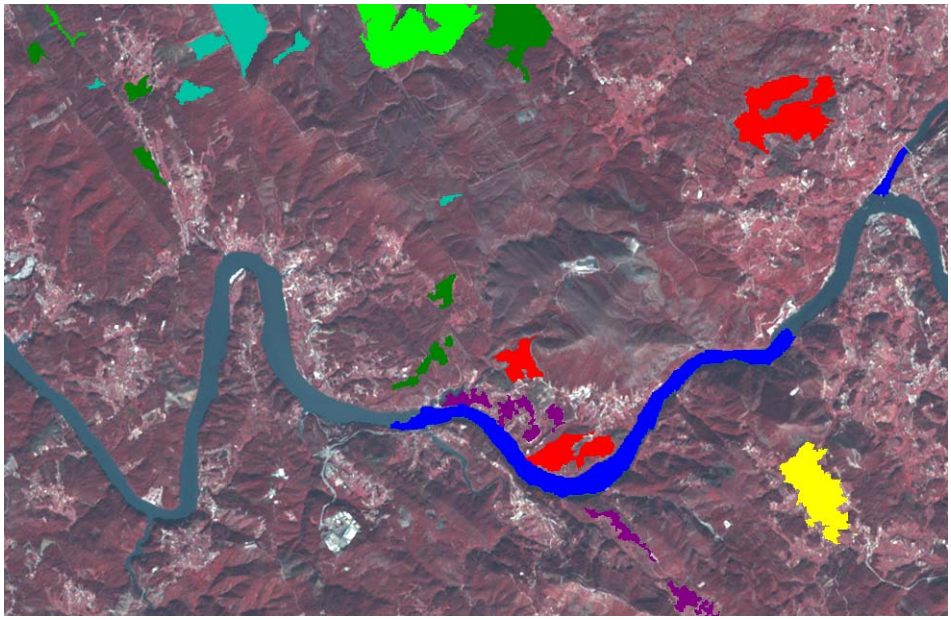

Figure 3. Section of the ASTER image with some of the training areas

identified for training. Table 1 shows the average size and number of objects used for training each class. Unfortunately only a small number of objects were available for some of the classes, because they appear sparsely in the study area.

Classification results

The classification of the ASTER 'mosaic' image was performed on eCognition software, using a method based on fuzzy logic (Baatz et al, 2001). A given object is assigned a probability value (p_i) to belong to class i. The object will have information about the 3 classes (i_{1st}, i_{2nd}, i_{3rd}) with highest probabilities and their values (p_{1st}, p_{2nd}, p_{3rd}). The class assigned will be that with higher probability value. The value of p_{1st} is one indication of how reliable the classification result is. Another and perhaps more consistent indicator is the stability $\Delta p = p_{1st} - p_{2nd}$. In the best-case scenario we would have $p_{1st}=1$ and $p_i=0$ for all the other classes ($i \neq i_{1st}$). That would result in a categorical choice of the object class and the value for Δp would be 0. On the opposite case we would have $p_{1st}=p_{2nd}$ and that would result in $\Delta p=0$. A summary of the main classification results is presented on Table 2. The number of objects assigned to each class varied form only 197 for 'Water' (HH) to over 19000 for 'Urban' (SC). It is worth pointing that, according to the training areas, the average object size for 'Water' was about 8 times larger than for 'Urban', who has the lowest average object size. The mean value of p_{1st} is high for all classes (above 95%) that suggest that in general the main classes present in the image were those looked for. However, the stability indicator is not very good for most classes. The mean difference between the highest and the second highest probability is 0.15 and 0.13 for the classes 'Urban' and 'Water', and around 0.05 (5%) for the classes 'Agricultural' (AG) and 'Burned areas' (FOGO). Although these values are not very high, they suggest that on average the objects assigned to these classes are likely to be well classified. For the remaining classes the mean stability is 0.01 (1%) or less which suggests that it is very likely that a significant number of these objects might not have been classified correctly.

Table 2. Fuzzy classification accuracy assessment

Class	No. of Objects	Mean p_{1st}	Mean Stability	Max Stability
SC	19180	0.956	0.152	1.00
HH	197	0.956	0.133	0.50
FOGO	1784	0.965	0.056	0.70
FlEcEc	2333	0.990	0.007	0.07
Flmix	6783	0.987	0.007	0.06
FlFdFd	1019	0.976	0.010	0.06
FlPbPb	2098	0.989	0.006	0.03
IC	3876	0.982	0.010	0.05
AG	12984	0.979	0.052	0.98

Figure 4. Section of the classified image

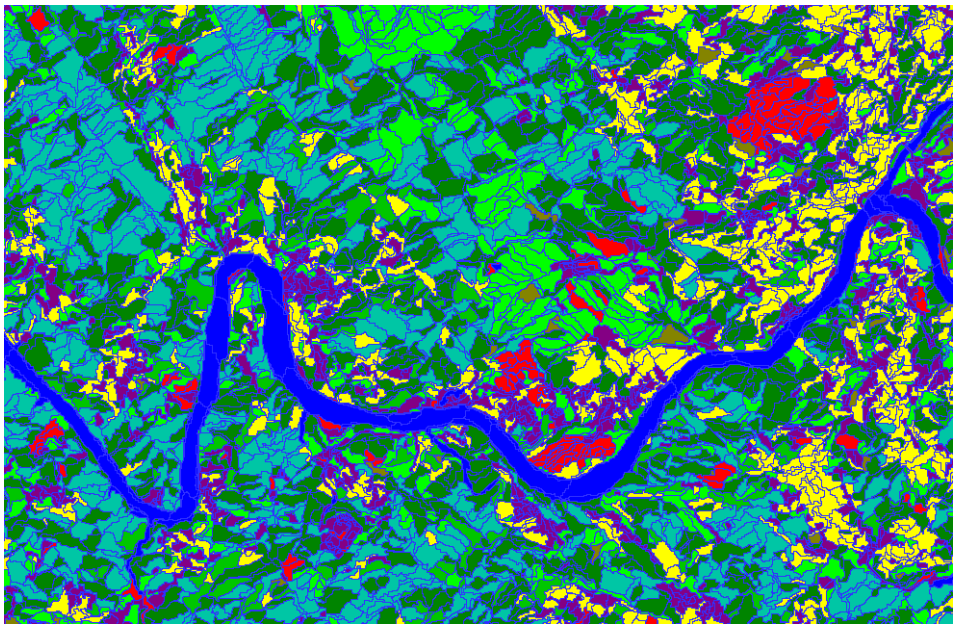

The image was classified at segmentation levels 1, 2 and 3. A section of the classified image at level 1 (smallest objects) is presented on Figure 4. The color key for the classes is the same as on Table 1.

Table 3. Summary of validation results

Class	No. sites	Level 1	Level 2	Level 3
SC	5	60.0%	80.0%	60.0%
HH	0	-	-	-
FOGO	3	100.0%	66.7%	66.7%
FlEcEc	54	37.0%	38.9%	33.3%
Flmix	68	54.4%	45.6%	51.5%
FlFdFd	0	-	-	-
FlPbPb	11	8.3%	0.0%	16.7%
IC	5	80.0%	80.0%	60.0%
AG	0	-	-	-
TOTAL	147	46.3%	42.2%	42.9%

Validation sites. An inspection of the existing cartography showed that the class 'Water' identified on the classified image perfectly matches the rivers. A number of independent test sites (point locations) were selected on the image. These sites were chosen in two areas of the Vale do Sousa region by applying a rectangular grid with intervals of around 800 meters. Only the points classified as one of the forest types in the 1995 land cover data were considered. A total of 335 test sites were identified. The land cover of 147 of these sites was obtained by ground inspection. The survey of the remaining sites is currently underway. Table 4 shows a summary of the validation results. According to the 1995 survey, every test site should have been one of the 'Forest' classes. However, 5 sites were in fact found to be 'Urban' (SC), 5 were 'Uncultivated' (IC) and 3 were 'Burned areas' (FOGO). The class 'Forest - Hardwoods' (FlFdFd) did not feature in any of the test sites surveyed so far, as this is the less common of all classes in the Vale do Sousa region. The average accuracy was only 46.3% for the image segmented at level 1, 42.2% for level 2, and 42.9% for level 3.

EVALUATION

The average accuracy of the classification is not satisfactory. The accuracy would certainly have been better if all 9 classes were used equally for the validation site selection. The spectral mixture between the various 'Forest' sub-classes is likely to be the main reason for the poor classification results, according to the stability values of the fuzzy classification.

Maximum likelihood classification on a pixel basis

A Maximum Likelihood classifier was applied to the ASTER image, using the same training areas, but on a pixel-by-pixel basis (PCI Geomatics, 2001). All 9 bands from the VNIR and SWIR were used. The confusion matrix for the 9 classes is presented on Table 4. The average accuracy was 73.36% and the overall accuracy was 71.50%. The confusion matrix shows that there is substantial mixture between the various 'Forest' classes. The class 'Uncultivated' (IC) is also not very well discriminated.

Table 4. Confusion Matrix for the supervised classification on a pixel-by-pixel basis.

d_{JM}	SC	HH	FOGO	FlEcEc	Flmix	FlFdFd	FlPbPb	IC	AG
SC	86.65 %	0.01 %	2.24 %	0.02 %	0.18 %	0.35 %	0.33 %	1.56 %	8.67 %
HH	0.98 %	97.45 %	0.02 %	0.00 %	0.10 %	0.81 %	0.09 %	0.53 %	0.02 %
FOGO	10.11 %	0.00 %	85.10 %	0.18 %	0.58 %	0.06 %	2.60 %	1.16 %	0.19 %
FlEcEc	2.24 %	0.00 %	0.31 %	75.92 %	10.45 %	6.15 %	1.70 %	3.05 %	0.18 %
Flmix	4.82 %	0.00 %	0.86 %	30.36 %	33.77 %	10.99 %	7.52 %	8.78 %	2.89 %
FlFdFd	6.52 %	0.07 %	0.28 %	5.81 %	6.73 %	63.95 %	0.78 %	10.34 %	5.52 %
FlPbPb	6.60 %	0.00 %	2.10 %	2.04 %	5.66 %	0.74 %	75.49 %	6.11 %	1.26 %
IC	12.83 %	0.00 %	1.95 %	3.70 %	8.54 %	6.24 %	4.32 %	59.59 %	2.84 %
AG	11.78 %	0.00 %	0.19 %	0.01 %	1.02 %	3.14 %	0.32 %	1.23 %	82.31 %

Class separability

The Jeffries-Matusita (J-M) distance is a good indicator of the separability between classes. The J-M distance between a pair of probability distributions (spectral classes) converges asymptotically to 2.0 as a function of the

distance between class means (Richards and Jia, 1999). In general, the larger the separability values between classes, the better the classification results should be. As a commonly used rule, the separability between two classes is considered good when the J-M distance is above 1.90. Two classes are considered to be very poorly separated when the J-M distance is below 1.0 (PCI Geomatics, 2001).

Table 5. Jeffries Matushita distance for 9 classes

d_{JM}	SC	HH	FOGO	FlEcEc	Flmix	FlFdFd	FlPbPb	IC
HH	2.00							
FOGO	1.68	2.00						
FlEcEc	1.95	2.00	1.95					
Flmix	1.89	2.00	1.88	0.42				
FlFdFd	1.85	2.00	1.91	1.25	0.84			
FlPbPb	1.90	2.00	1.82	1.49	1.02	1.63		
IC	1.82	2.00	1.75	1.40	0.96	1.06	1.36	
AG	1.57	2.00	1.91	1.92	1.74	1.58	1.88	1.71

The JM distance was computed for the 9 classes, from the training areas on a pixel-by-pixel basis. The results are presented on Table 5. As expected, the separability between 'Water' (HH) and all the other classes is excellent. The class 'Burned' (FOGO) is also well separated from most classes. The classes IC and SC are reasonably separated from each other, as is SC and the 4 'Forest' sub-classes. The main problems occur between the various 'Forest' sub-classes and between these and IC.

Table 6. Jeffries Matushita distance for 6 classes

d_{JM}	SC	HH	FOGO	FL	IC
HH	2.00				
FOGO	1.68	2.00			
FL	1.90	2.00	1.87		
IC	1.82	2.00	1.75	1.03	
AG	1.57	2.00	1.91	1.77	1.71

The four 'Forest' sub-classes were merged into a single class. The J-M distance computed for the resulting 6 classes, presented on Table 6, shows a much better separability between classes. The single low J-M distance value is between 'Forest' (FL) and 'Uncultivated' (IC).

Unsupervised classification with hierarchical clustering

The unsupervised classification algorithm ISODATA was applied to the ASTER image (PCI Geomatics, 2001). A total of 33 classes were obtained after 147 iterations when the classifier converged. These classes can be thought of as probability density clusters in the multi-spectral space. Ideally each one of the classes characterized in the training areas would correspond to one of these clusters, or perhaps more than one clusters close together in the multi-spectral space. A comparison between the 9 land cover classes and the clusters from the unsupervised classification was carried out to evaluate the spectral similarity between classes. The 33 clusters were structured hierarchically according to their relative distance. Figure 5 shows the hierarchic structure of 25 of these clusters, labeled from A to Y. The cluster X is an aggregation of 4 original clusters all related to non-observed areas of the image. The reason that non-observed pixels were assigned 4 different clusters has to do with slight different coverage by the VNIR and SWIR instruments. Another 7 clusters from the original 33 were aggregated into clusters W and Y as the number of pixels from the training areas in these clusters was negligible. On Figure 5 it is also shown the correspondence between the land cover classes, based on the training areas, and the clusters identified by the unsupervised classification. For example, 8790 of the 8936 pixels (98.4%) identified as 'Water' in training belong to cluster I. This is represented in Figure 5 in blue with a solid square (91-100%). The class 'Water' is very well defined in the multi-spectral space, not only because it is mostly associated with a single cluster, but also because this cluster only merges with others at a quite high level in the hierarchy tree. Another

good example is 'Agricultural' (AG). Although most of the pixels identified in this class in training (74.4%) belong to 4 different clusters (O, P, Q and R), these clusters would merge amongst themselves first, by moving upwards in the hierarchical tree.

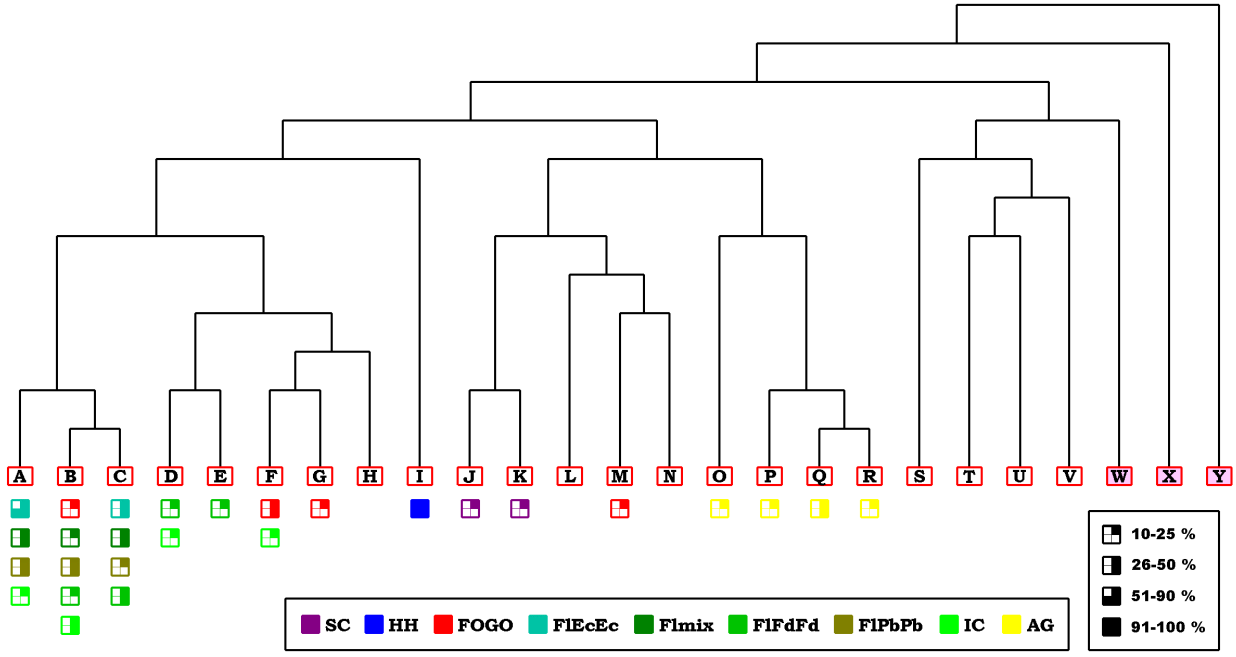

An example of a class poorly characterized spectrally is 'Burned areas' (FOGO). Over 91% of the pixels from the training of this class belong to 4 clusters (B, F,G and M), but, unlike 'Agricultural', these clusters are far apart in the tree. In order to have them all merged together an aggregation of 18 clusters would have to be done. Furthermore, cluster B is shared with several other classes.

As Figure 5 shows, the 'Forest' sub-classes are reasonably well defined in the multi-spectral space. The problem with these classes is that they all share the same multi-spectral space / clusters. It is therefore impossible to clearly discriminate between them. This is again consistent both with the ground validation results and the J-M distance values.

CONCLUSIONS

The classification of a multi-spectral image segmented into objects should provide more realistic result results than treating pixels as individual observations, independently from their neighborhood. The pixel is in many cases a too small unit, and its fixed size is also a limitation. Fuzzy classification methods also provide realistic results, but when only the 1st score is considered the benefits of this method are somehow lost.

A practical application of object based supervised classification was undertaken on an ASTER satellite image, with the purpose of land cover update. The classification accuracy was checked by confusion matrix and by validation from ground surveys. The training data was evaluated by separability measurements and hierarchical clustering. Land cover classes of various Forest types were found difficult to discriminate, mainly due to their spectral similarity.

ACKNOWLEDGEMENTS

The authors wish to thank the ASTER ERSDAC for providing the satellite data through an Announcement of Research Opportunity (ARO-070).

REFERENCES

Baatz, M., Benz, U., Dehghani, S., Heynen, M., Höltje, A., Hofmann, P., Lingenfelder, I., Mimler, M., Sohlbach, M., Weber, M., Willhauck, G. (2001). eCognition Object Oriented Image Analysis. User Guide, Definiens Imaging, München, Germany.

ERSDAC (2000). DAR Guideline – Guide for ASTER ARO users: How to Submit "Data Acquisition Requests", Version 1.0. Earth Remote Sensing Data Analysis Center, ASTER ARO Office, Tokyo, Japan.

PCI Geomatics (2000). Ortho Engine Reference Manual, Version 7.0. PCI Geomatics, Ontario, Canada.

PCI Geomatics (2001). X-Pace Reference Manual, Version 8.2. PCI Geomatics, Ontario, Canada.

Richards, J.A., Jia, X. (1999). *Remote Sensing Digital Image Analysis - An Introduction.* Third Edition, Springer-Verlag.

Tomé, M., Fidalgo, B., Gaspar, J. (2002). Normas de fotointerpretação para as áreas de demonstração da Associação Florestal do Vale do Sousa. Relatórios Técnicos do GIMREF, No.1/2002, Universidade Técnica de Lisboa, Instituto Superior de Agronomia, Lisboa, Portugal.

Yamaguchi, Y., Kahle, A. B., Tsu, H., Kawakami, T., Pniel, M. (1998). Overview of Advanced Spaceborne Thermal Emission and Reflection Radiometer (ASTER). *IEEE Transactions on Geoscience and Remote Sensing*, *36*(4):1062-1071.